

Measurements of $t\bar{t}$ production cross-sections with the ATLAS experiment at the LHC

M. Spalla^{1*}, on behalf of the ATLAS Collaboration¹.

¹ Max-Planck-Institut für Physik (Werner-Heisenberg-Institut), München, Germany

* margherita.spalla@cern.ch

July 27, 2021



*Proceedings for the XXVIII International Workshop
on Deep-Inelastic Scattering and Related Subjects,
Stony Brook University, New York, USA, 12-16 April 2021*
doi:[10.21468/SciPostPhysProc.202103001](https://doi.org/10.21468/SciPostPhysProc.202103001)

Abstract

Comprehensive measurements of differential cross-sections of top-quark-antiquark pair-production are presented. They are performed in the dilepton, lepton+jets and the all-hadronic channels, using $\sqrt{s} = 13$ TeV data from the ATLAS detector at the LHC. Several setups of next-to-leading order and next-to-next-to-leading order generators are quantitatively compared to the measurements. In addition, total cross-section measurements using up to the full ATLAS Run 2 dataset are presented.

1 Introduction

The production of a top and an anti-top pair ($t\bar{t}$) is the dominant channel for top-quark production in proton-proton collisions at the Large Hadron Collider (LHC). The very large statistics of $t\bar{t}$ pairs produced at the LHC allows for percent level precision in the measurement of $t\bar{t}$ cross-sections, through multiple complementary decay channels and phase space regions.

Precise $t\bar{t}$ measurements are a very powerful tool for testing the Standard Model, by accurately probing QCD in the high energy region. Measurements of the $t\bar{t}$ cross-section are also sensitive to the value of fundamental Standard Model parameters, such as the top-quark mass, as well as potential Beyond the Standard Model signals. Finally, $t\bar{t}$ production is a major background to multiple important Standard Model and Beyond the Standard Model signals.

The $t\bar{t}$ production has been studied extensively at the ATLAS Experiment [1], through multiple differential and double differential cross-section measurements, as well as inclusive cross-section results.

2 Differential Cross-Section measurements

Differential $t\bar{t}$ cross-section at $\sqrt{s} = 13$ TeV has been measured in the dilepton, lepton(ℓ)+jets and all-hadronic decay channels. Multiple kinematic variables have been used for both differential and double differential cross-sections.

¹Copyright 2021 CERN for the benefit of the ATLAS Collaboration. Reproduction of this article or parts of it is allowed as specified in the CC-BY-4.0 license.

The uncertainty on most of the presented measurements is dominated by systematic sources. Monte Carlo modelling of signal and background is often one of the largest uncertainty components, other large sources are experimental (e.g. lepton identification, jet energy calibration) or associated to data-driven background description. To reduce the impact of systematic uncertainties, differential distributions are mostly normalised to the inclusive cross-section.

2.1 Dilepton channel

The dilepton channel analysis [2] ($L = 36.1 \text{ fb}^{-1}$) focuses on events with an opposite-sign electron-muon pair in association with 1 or 2 b-tagged jets. Differential and double differential cross-sections are evaluated as a function of lepton kinematic variables, without fully reconstructing the $t\bar{t}$ system. The cross-section is extracted in every bin, by interpolating the number of events with 1 and 2 b-tagged jets. This method reduces the impact of uncertainties on jet b-tagging and calibration.

Results are compared to multiple NLO + parton-shower Monte Carlo simulations, differing in e.g. matrix-element generator, parton-shower, factorisation and renormalisation scales or PDF set. Overall, good agreement between data and simulation is observed. The simulation is found to poorly describe the data in some kinematic regions, such as high lepton transverse momentum (p_{\perp}), as shown in Figure 1a.

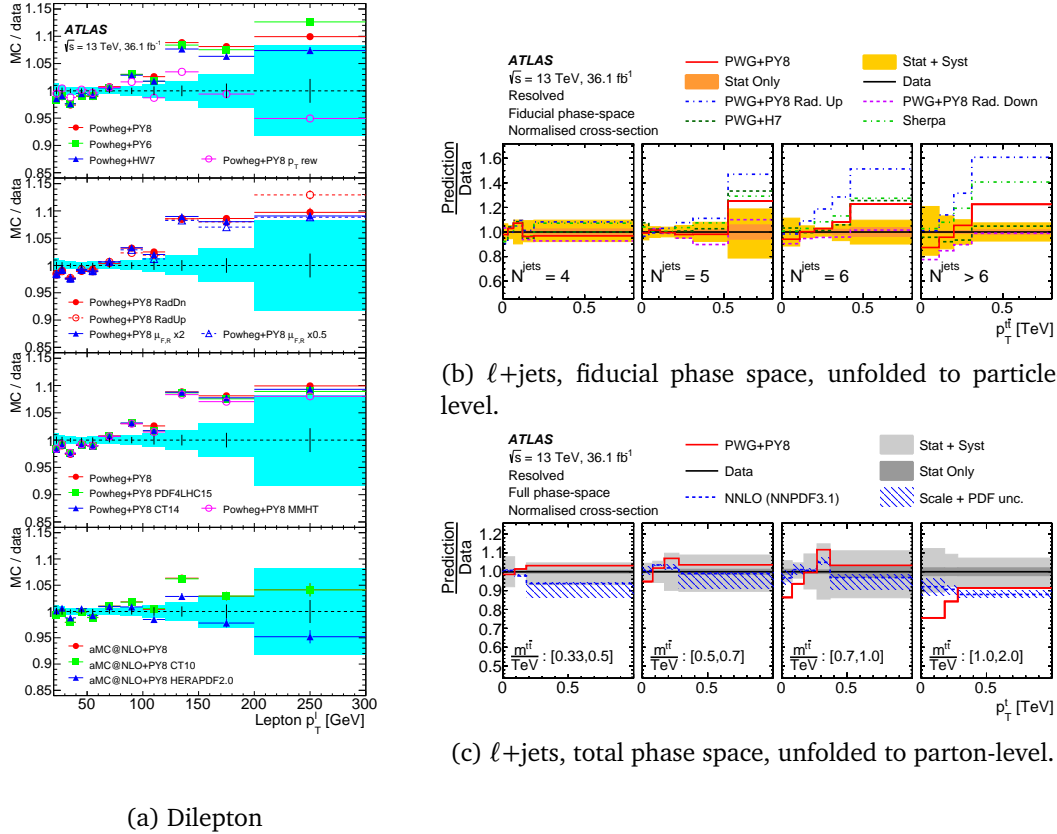


Figure 1: Ratios of predictions of normalised differential cross-sections to data as a function of kinematic variables. a: di-lepton channel [2], cross-section as a function of the lepton p_{\perp} , compared to particle-level prediction. b (c): ℓ +jets channel [3], cross-section in the fiducial (total) phase space, as a function of the p_{\perp} of the $t\bar{t}$ pair (top-quark p_{\perp}) in bins of the number of jets ($t\bar{t}$ invariant mass).

2.2 ℓ +jets channel

The analysis in the ℓ +jets channel [3] is also based on 36.1 fb^{-1} of data. Two topologies are considered, respectively requiring a *resolved* and a *boosted* hadronic top-quark². A comparison between the results in the two topologies shows good agreement between the boosted and the resolved channel. The selected jets, lepton, and missing transverse momentum are used to reconstruct the $t\bar{t}$ four-momenta. Data are then unfolded to both fiducial (particle-level) and total (parton-level) phase space. The boosted channel remains limited to the region of high top-quark transverse momenta, to avoid too large extrapolation uncertainties.

Results in the fiducial phase space are compared to multiple Monte Carlo predictions. The simulation is for the most part in good agreement with data, even though poor agreement is observed in some phase space regions. Similarly to the case of the dilepton channel, the predicted p_{\perp} spectrum tends to be too hard, an example is shown in Figure 1b.

The ℓ +jets results in the full phase space allow a direct comparison to NNLO+NNLL calculation. The NNLO calculation improves over NLO + parton-shower simulation, except for a few regions of the phase space, such as high top p_{\perp} and high $t\bar{t}$ mass as in Figure 1c.

2.3 All-hadronic

The most recent result in the all-hadronic channel is a resolved analysis [4], requiring 6 resolved jets and no leptons. The $t\bar{t}$ is fully reconstructed, thanks to the absence of direct neutrinos from W boson decays. This improves the kinematic resolution with respect to the ℓ +jets

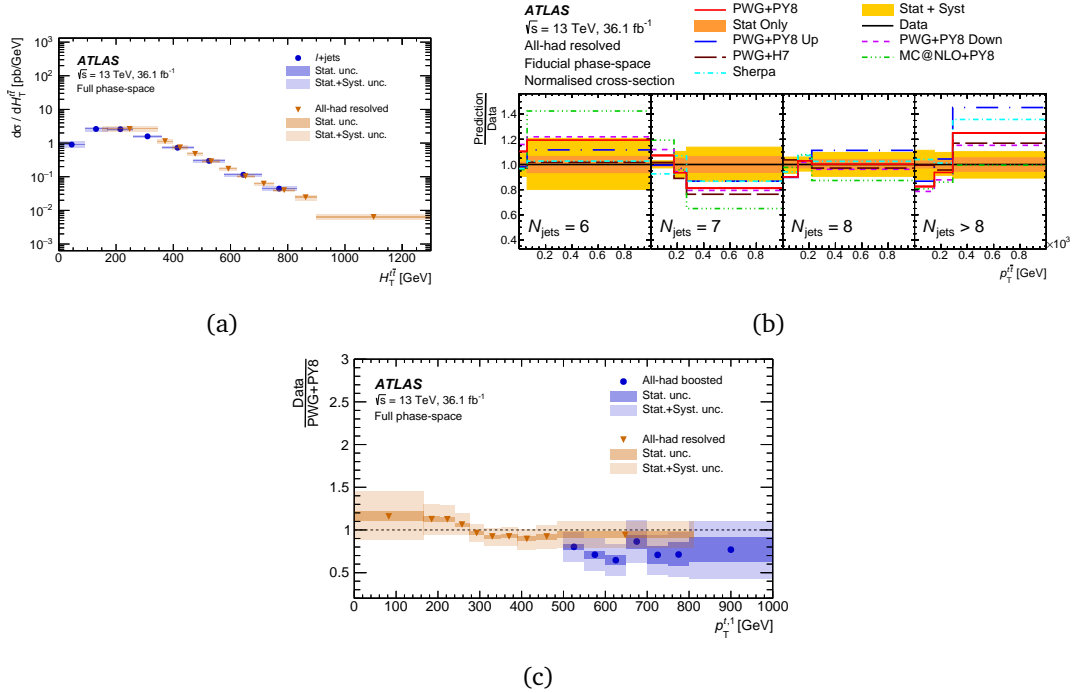


Figure 2: a: Comparison between the measured differential cross-sections at parton-level, in the ℓ +jets and all-hadronic channels, as a function of the scalar sum of the top-quarks p_T ($H_T^{\bar{t}\bar{t}}$). b: Ratio of the measured parton-level differential cross-sections to Monte Carlo predictions in the all-hadronic resolved and boosted topologies. c: Double-differential normalised cross-section at particle-level, as a function of the $t\bar{t}$ pair transverse momentum in bins of the jet multiplicity. From [4].

²An hadronic top-quark is referred to as *resolved* when its decay products can be reconstructed as separate jets. A *boosted* top-quark results in collimated decay products and is reconstructed as a single jet of large radius.

channel, counter-balancing the large multi-jet background that characterises the all-hadronic final state. Figure 2a shows the $t\bar{t}$ differential cross-section in the resolved all-hadronic and ℓ +jets channels, unfolded to parton-level in the total phase space. The two measurements are in very good agreement with each other and provide similar precision.

In order to study the all-hadronic differential cross-section in the fiducial phase space, a set of $t\bar{t}$ kinematic variables similar to the ℓ +jets one has been chosen. A comparison with predictions from multiple generators provides in general good agreement. Data over Monte Carlo ratios are mostly consistent with what has been observed in the ℓ +jets channel, even though different behaviours are seen for some variables, an example is shown in Figure 2b.

The all-hadronic analysis also extensively studies the effect of additional jet radiation. The differential cross-section is measured as a function of multiple transverse momentum ratios, between top-quarks and additional jets in the event.

An earlier measurement of the all-hadronic $t\bar{t}$ cross-section required both top-quarks to be boosted [5]. Measured differential cross-sections in the boosted and resolved all-hadronic channels are compared in Figure 2c, indicating good agreement between the two kinematic regions. Measurements in the all-hadronic boosted channel are generally well modelled, though uncertainties tend to be larger than for the ℓ +jets boosted analysis.

3 Inclusive cross-section

Inclusive $t\bar{t}$ cross-section measurements complement the differential results. For both the all-hadronic and dilepton measurements, the inclusive cross-section is extracted in the same way as the differential one, except for all events being grouped in a single bin.

In the ℓ +jets channel, on the other hand, a separate inclusive cross-section measurement has been performed, using the full Run 2 dataset of 139 fb^{-1} [6].

The cross-section is extracted through a simultaneous profile-likelihood fit in 3 signal regions, which vary in sensitivity to the modelling of b-jets and jet multiplicity.

Inclusive $t\bar{t}$ cross-section measurements in the total phase space are summarised in Table 1, together with the prediction (referenced in [6]) from NNLO+NNLL calculation with Top++ [7]. Results are in agreement both with one another and with the NNLO+NNLL prediction. Best precision is reached in the dilepton channel.

Ratios between cross-sections measured at 13 TeV and 7 or 8 TeV have been computed in the dilepton channel, as well as double ratios of $t\bar{t}$ to Z production cross-sections, at 13 and 7 / 8 TeV. The theoretical prediction overestimates both single and double 13 to 7 TeV ratio by about 1σ , while it underestimates the 13 to 8 TeV ratios by roughly the same amount.

Finally, an indirect measurement of the top-quark pole mass is extracted by fitting the inclusive dilepton cross-section. It is found to be $m_t^{\text{pole}} = 173.1_{-2.1}^{+2.0} \text{ GeV}$, consistent with other m_t^{pole}

$\sigma_{t\bar{t}}$ [pb]	Uncertainty [pb]	Channel
830	± 0.4 (stat.) ± 36 (syst.) ± 14 (lumi.)	ℓ +jets, 139 fb^{-1} , resolved [6]
826.4	± 3.6 (stat) ± 11.5 (syst) ± 15.7 (lumi) ± 1.9 (beam)	Dilepton, 36.1 fb^{-1} [2]
864	± 127 (stat. + syst.)	All-had., 36.1 fb^{-1} , resolved [4]
832	$^{+20}_{-29}$ (scale) ± 35 (PDF, α_s)	NNLO+NNLL (referenced in [6])

Table 1: Comparison between the $t\bar{t}$ inclusive cross-section measurements discussed here, as well as the prediction from NNLO+NNLL calculation.

measurements.

The dilepton inclusive cross-section has also been measured at $\sqrt{s} = 5.02 \text{ TeV}$, using 257 pb^{-1}

of data [8]. Selected events contain an opposite sign lepton pair, the $e\bar{e}$ and $\mu\bar{\mu}$ channels are included to improve the statistics. The cross-section is extracted through a similar procedure to the 13 TeV dilepton analysis. The measured cross-section is: $\sigma_{t\bar{t}}(5.02 \text{ TeV}) = 66.0 \pm 4.5 \text{ pb}$, in agreement with the Top++ NNLO+NNLL prediction of $68.2 \pm 4.8(\text{PDF}, \alpha_s)_{-2.3}^{+1.9}(\text{scale}) \text{ pb}$ [8].

4 Conclusion

An extensive program of precision $t\bar{t}$ cross-section measurements has been carried out by the ATLAS experiment at the LHC. Results reach comparable or better precision than the available Standard Model prediction.

The existing predictions provide in general good agreement with data, even though poorer modelling is observed in some kinematic regions, such as high p_{\perp} . These discrepancies could be explained by missing higher order contributions and point towards the need for further studies with improved simulation. Results are mostly consistent throughout measurements.

References

- [1] The ATLAS Collaboration, *The ATLAS experiment at the CERN Large Hadron Collider*, JINST 3 (2008), doi:[10.1088/1748-0221/3/08/s08003](https://doi.org/10.1088/1748-0221/3/08/s08003).
- [2] The ATLAS Collaboration, *Measurement of the $t\bar{t}$ production cross-section and lepton differential distributions in $e\mu$ dilepton events from pp collisions at $\sqrt{s} = 13 \text{ TeV}$ with the ATLAS detector*, Eur. Phys. J. C 80, 528 (2020), doi:[10.1140/epjc/s10052-020-7907-9](https://doi.org/10.1140/epjc/s10052-020-7907-9), [arXiv:1910.08819](https://arxiv.org/abs/1910.08819).
- [3] The ATLAS Collaboration, *Measurements of top-quark pair differential and double-differential cross-sections in the ℓ +jets channel with pp collisions at $\sqrt{s} = 13 \text{ TeV}$ using the ATLAS detector*, Eur. Phys. J. C 79, 1028 (2019), doi:[10.1140/epjc/s10052-019-7525-6](https://doi.org/10.1140/epjc/s10052-019-7525-6), [Erratum: Eur.Phys.J.C 80, 1092 (2020)], [arXiv:1908.07305](https://arxiv.org/abs/1908.07305).
- [4] The ATLAS Collaboration, *Measurements of top-quark pair single- and double-differential cross-sections in the all-hadronic channel in pp collisions at $\sqrt{s} = 13 \text{ TeV}$ using the ATLAS detector*, JHEP 01, 033 (2021), doi:[10.1007/JHEP01\(2021\)033](https://doi.org/10.1007/JHEP01(2021)033), [arXiv:2006.09274](https://arxiv.org/abs/2006.09274).
- [5] The ATLAS Collaboration, *Measurements of $t\bar{t}$ differential cross-sections of highly boosted top quarks decaying to all-hadronic final states in pp collisions at $\sqrt{s} = 13 \text{ TeV}$ using the ATLAS detector*, Phys. Rev. D 98, 012003 (2018), doi:[10.1103/PhysRevD.98.012003](https://doi.org/10.1103/PhysRevD.98.012003), [arXiv:1801.02052](https://arxiv.org/abs/1801.02052).
- [6] The ATLAS Collaboration, *Measurement of the $t\bar{t}$ production cross-section in the lepton +jets channel at $\sqrt{s} = 13 \text{ TeV}$ with the ATLAS experiment*, Phys. Lett. B 810, 135797 (2020), doi:[10.1016/j.physletb.2020.135797](https://doi.org/10.1016/j.physletb.2020.135797), [arXiv:2006.13076](https://arxiv.org/abs/2006.13076).
- [7] M. Czakon and A. Mitov, *Top++: A program for the calculation of the top-pair cross-section at hadron colliders*, Computer Physics Communications 185, 2930–2938 (2014), doi:[10.1016/j.cpc.2014.06.021](https://doi.org/10.1016/j.cpc.2014.06.021).
- [8] The ATLAS Collaboration, *Measurement of the $t\bar{t}$ production cross-section using dilepton events in pp collisions at $\sqrt{s} = 5.02 \text{ TeV}$ with the ATLAS detector*, ATLAS-CONF-2021-003 (2021), <https://cdsweb.cern.ch/record/2754223>